Quark propagators in confinement and deconfinement phases

Masatoshi Hamada,[1] Hiroaki Kouno,[2] Atsushi Nakamura,[3] Takuya Saito,[4] and Masanobu Yahiro[1]
[1]*Department of Physics, Kyushu University, 6-10-1 Hakozaki, Higashi-ku, Fukuoka, 812-8581, Japan*
[2]*Department of Physics, Saga University, 1 Honjyo-cho, Saga, 840-8502, Japan*
[3]*Information Media Center, Hiroshima University, 1-7-1 Kagami-yama, Higashi-hiroshima, 739-8521, Japan*
[4]*Integrated Information Center, Kochi University, 2-5-1, Akebono-cho, Kochi, 780-8520, Japan*
(Received 21 February 2010; published 27 May 2010)

We study quark propagators near the confinement/deconfinement phase transition temperature in quenched-lattice simulation of QCD. We find that there is no qualitative change for the quark propagators in both phases. In the confinement phase, those effective quark masses in units of the critical temperature behave as a constant as a function of the temperature, while above the critical temperature, the value of the effective quark mass drops to circa half value.

DOI: 10.1103/PhysRevD.81.094506 PACS numbers: 12.38.Gc, 12.38.Mh, 21.65.Qr

I. INTRODUCTION

Quarks are confined in hadrons in the usual environment, i.e., at zero temperature and density. All the quarks, $u, d, s, \ldots,$ are always confined in hadrons in the low-energy region.

Lattice quantum chromodynamics (QCD) calculations predict that quarks are deconfined at a critical temperature [1]: Polyakov loop, which corresponds infinitely heavy quark, changes from zero to finite as the temperature increases.

At the Relativistic Heavy-Ion Collider (RHIC), the temperature of the produced matter may exceed the phase transition temperature, T_c. The realization of quark-gluon plasma (QGP) is argued in many phenomenological analyses [2]. The results of the phenomenological, experimental, and theoretical studies strongly suggest that in the RHIC temperature region; QGP is not a free quark-gluon gas, but the quarks and gluons strongly interact with each other [3]. It is now highly desirable to investigate the detailed characteristics of the QGP matter near the confinement-deconfinement transition temperature.

One of the most basic quantities of QCD is a quark propagator, whose behavior in the infrared region is significantly related to the chiral symmetry breaking. This causes chiral condensation to be an order parameter, $\langle \psi(x)\bar{\psi}(x)\rangle$, which is the scalar part of the quark propagators at the same coordinate point. The condensation plays a role of an effective mass of quarks, and explains the phenomenological pictures of quarks: constituent quark masses, quark confinement at large distances.

The confinement of quarks means that the asymptotic state of quarks is not observed. It is then expected that the confining quarks have no single-pole mass. These are characteristic phenomena for hadron physics and thus have attracted interest of many researchers who study the behavior of the quark propagators by the Schwinger-Dyson approaches [4–7] as well as the lattice QCD calculations [8–15]. On the other hand, the chiral symmetry is restored in the QGP phase where quarks are deconfined. It is thus natural to expect that the quark property changes drastically after the QGP phase transition. Moreover, in the RHIC temperature region, quark propagators are not necessarily those of a free particle because they may interact strongly with gluons. Therefore, it is important to clarify how quarks behave in a heat bath, particularly near the critical temperature T_c, in comparison with those in the confinement phase. For thermal quarks, some works were made so far by using lattice QCD [16–18]. Particularly in Ref. [18], extensive analyses were made for spectral properties of quarks about particle/hole excitation in the QGP phase. We here focus our analyses on temperature dependence of quark propagators in both the confinement and deconfinement phases in order to reveal their confinement properties.

In this study, we calculate quark propagators using quenched-lattice QCD simulation in the Landau-gauge fixing. In Sec. II the general discussions of them are given and numerical results are shown in Sec. III. Section IV is devoted to a summary.

II. QUARK PROPAGATORS BELOW AND ABOVE THE PHASE TRANSITION TEMPERATURE

A. Time-time correlation function

Quark propagators may be written as

$$G(\vec{p}=0, p_4) = \frac{Z(p_4)}{ip_4\gamma_4 + m} = \frac{Z(p_4)(-ip_4\gamma_4 + m)}{p_4^2 + m^2}, \quad (1)$$

if they have a single pole, where m is the pole mass, Z is the renormalization function, and p_4 is the fourth component of momentum. The time-time correlation function in the coordinate space is defined as

$$G(t) \equiv \langle \psi(t)\bar{\psi}(0)\rangle = \sum_{p_4} G(p_4)e^{ip_4 t}. \quad (2)$$

After taking the sum over Matsubara frequencies, $p_4 = \pi(2n+1)\beta$, Eq. (2) together with Eq. (1) becomes

$$G(t) = \frac{C}{\cosh(m\beta/2)} \times [\cosh(m(t-\beta/2))\gamma_4 - \sinh(m(t-\beta/2))], \quad (3)$$

where $\beta = 1/T$ is the temporal-lattice size and C is a constant.

In Källen-Lehmann spectral representation, propagators are written as the sum of a one-pole function,

$$G(t) = \int dm^2 \frac{\rho(m^2)}{i\not{p}_\mu + m}. \quad (4)$$

In addition, the form of a time-time correlation function of $\vec{p} = 0$ is written as

$$G(t) = G_4(t)\gamma_4 + G_s(t). \quad (5)$$

B. Quark Propagators

The quark propagator is written as an inverse fermion matrix in the lattice QCD formulation,

$$G^{ab}_{\alpha\beta}(x, y) = \langle \psi^a_\alpha(x)\bar{\psi}^b_\beta(y)\rangle = \langle W^{-1}(x, y; U)^{ab}_{\alpha\beta}\rangle, \quad (6)$$

where x and y are four-dimensional coordinates and U is the link variable. Here, a and b are color indices and α and β are Dirac indices. The fermion matrix is defined by a fermion action,

$$S_f = \sum_{x,y} \bar{\psi}(x)W(x, y; U)\psi(y), \quad (7)$$

where color and Dirac indices are suppressed. In this paper, S_f is the $\mathcal{O}(a)$-improved Wilson-fermion action [19], which reduces the lattice discretization artifact.

The time-time correlation function is written, using Eq. (6), as

$$G(x_4 - y_4) = \langle \psi(x_4)\bar{\psi}(y_4)\rangle = \sum_{\vec{x},\vec{y}} \langle W^{-1}(x, y; U)\rangle, \quad (8)$$

where x_4 and y_4 represent Euclidean-time components and $\vec{x}$ and $\vec{y}$ do spatial components. Equation (8) is decomposed into G_4 and G_s in Eq. (5).

Effective masses, $m(t)$, for vector and scalar parts are defined through the following ratios:

$$\frac{G_4(t)}{G_4(t+1)} = \frac{\cosh(m(t)(t-\beta/2))}{\cosh(m(t)(t+1-\beta/2))}, \quad (9)$$

$$\frac{G_s(t)}{G_s(t+1)} = \frac{\sinh(m(t)(t-\beta/2))}{\sinh(m(t)(t+1-\beta/2))}. \quad (10)$$

C. Deconfinement phase

In the deconfinement phase, the quarks are expected to become a physical particle, and a quasiquark state exists in the deconfinement phase if the thermal asymptotic state can be defined. This is because, above T_c, the Polyakov line expectation values increase from that at $T = 0$, and the energy density and the pressure of quark/gluon sector become finite. However, as pointed out first in Ref. [20], hadrons seem to survive even above T_c. Indeed, the Polyakov loops do not saturate. In this temperature region, the system is conjectured as a "semi-QGP" state, where partial confinement exists [21]. The shear viscosity predicted by lattice QCD is very small [22], which means that the interactions are very strong. New pictures based on the magnetic degrees of freedom, which originate from topological characters of QCD, are proposed to explain the nontrivial nature of these temperature regions [23–25].

In the following, therefore, we *assume* that the quasiparticle state exists. We will investigate whether this assumption holds by measuring the quark propagators in the deconfinement phase *and* in the confinement phase. In the latter, this assumption should be violated. By comparing the behavior of the quarks in two circumstances, we expect to reveal their features.

A quasistate has an energy gap from the thermal vacuum. This energy gap is called the thermal mass. It is defined as the pole of propagators. We obtain the mass from the flat values of the lattice time dependence of the effective mass.

D. Confinement Phase

A free quark state cannot exist in the confinement phase. Then, how does this confinement character appear in the quark propagators ? There are three possibilities:

(I) Numerical results in this phase can not be fitted by a single-pole ansatz.
(II) Single-pole fitting is applicable, but obtained quark mass is infinite (numerically very large).
(III) Quark propagators include negative norm state, that is, asymptotic states do not exist.

Since we employ the Landau gauge, there is no guarantee that $\rho(m)$ in Eq. (4) is positive definite; see Ref. [26] and also Sec. III of Chapter 4 in the lecture book by Nakanishi and Ojima [27]. When we analyze numerical data, we should keep in mind this possibility, and should not confuse the Case III with the first one, Case I.

III. NUMERICAL RESULT

We calculate quark propagators in quenched $SU(3)$ lattice simulation in the confinement and deconfinement phases. Gauge configurations are generated by the heat-bath method with the Wilson-plaquette gauge action. The gauge configurations updated are fixed by the Landau-gauge condition satisfying

$$\sum_a \left| 2\,\mathrm{Im}\,\mathrm{Tr}\frac{\lambda_a}{2}\sum_\mu (U_\mu(x) - U_\mu(x-\hat{\mu}))\right|^2 \leq 10^{-20} \quad (11)$$

TABLE I. Simulation parameters: lattice coupling $\beta = 6/g^2$, temporal-lattice length N_t, spatial lattice length N_s, temperature in units of critical temperature T/T_c (T_c depends on N_t), hopping factor κ, clover coefficient $C_{\rm SW}$ estimated nonperturbatively in Ref. [28]. For $\beta = 6.10$, 6.25, 6.32 and 6.47, the lattice cutoffs are approximately 0.088, 0.070, 0.064 and 0.052 [fm], respectively, which are estimated from the data of Ref. [29].

β	N_t	N_s	T/T_c	κ	$C_{\rm SW}$
6.10	8	24	1.08998	0.1345559	1.6787
6.10	8	24	1.08998	0.1353591	1.6787
6.10	16	24	0.54499	0.1345559	1.6787
6.10	16	24	0.54499	0.1353591	1.6787
6.10	6	32	1.45331	0.1345559	1.6787
6.10	8	32	1.08998	0.1345559	1.6787
6.10	10	32	0.871984	0.1345559	1.6787
6.10	12	32	0.726653	0.1345559	1.6787
6.10	14	32	0.622846	0.1345559	1.6787
6.25	8	24	1.36650	0.1346226	1.5876
6.25	8	24	1.36650	0.1352633	1.5876
6.25	8	32	1.36650	0.1346226	1.5876
6.25	16	24	0.68325	0.1346226	1.5876
6.25	16	24	0.68325	0.1352633	1.5876
6.25	16	32	0.68325	0.1346226	1.5876
6.32	8	24	1.51094	0.1346220	1.5560
6.32	8	24	1.51094	0.1352011	1.5560
6.32	16	24	0.75547	0.1346220	1.5560
6.47	8	24	1.85949	0.1345722	1.5028
6.47	8	24	1.85949	0.1350420	1.5028
6.47	16	24	0.929745	0.1345722	1.5028

for all the lattice sites. We adopt the clover type improved Wilson-fermion action to obtain quark propagators. Our numerical parameters are summarized in Table I. We here use $35 \sim 50$ configurations for each computation.

A. Propagators and effective masses

Numerical results for the vector part G_4 and the scalar part G_s of the time-time correlation function are shown in Fig. 1. No singularities occur for the quarks, not only in the deconfinement phase, but also in the confinement phase. This is a surprising result; that is, the quark propagators seem to provide no information on the confinement.

We plot the effective masses defined by the vector part of quark propagators in the confinement phase in Fig. 2. They rise up from below; this is an indication of the negative metric which results in an ill-defined spectral function. Their values increase more rapidly at small t region than at large t region. As a result, our computation does not give a plateau in t at low temperature, while as T approaches T_c the effective masses appear to be a constant. One may conclude that quarks have no asymptotic state at low temperature, i.e., Case III in Sec. II D.

The effective mass data suffer from poor temporal resolution. Therefore, the large lattice simulations are desirable to get more concrete conclusion. It should be noticed, however, that physical length along t direction, $N_t a = 1/T$, is limited even if we employ a large lattice, although we can achieve a better temporal resolution by increasing N_t and decreasing the lattice spacing a.

Note that the quark masses in our calculation are heavy, but this is not a reason for observing no clear signal of the confinement, because even heavy quarks are confined.

For the deconfinement phase, Fig. 3 shows that the effective masses also approach their asymptotic values from below with the imaginary time. It is difficult, however, to conclude an unphysical behavior of quark propagators in the deconfinement phase because this observation relies on only a few data points, and our lattice resolution along the temperature direction does not allow us to go any further.

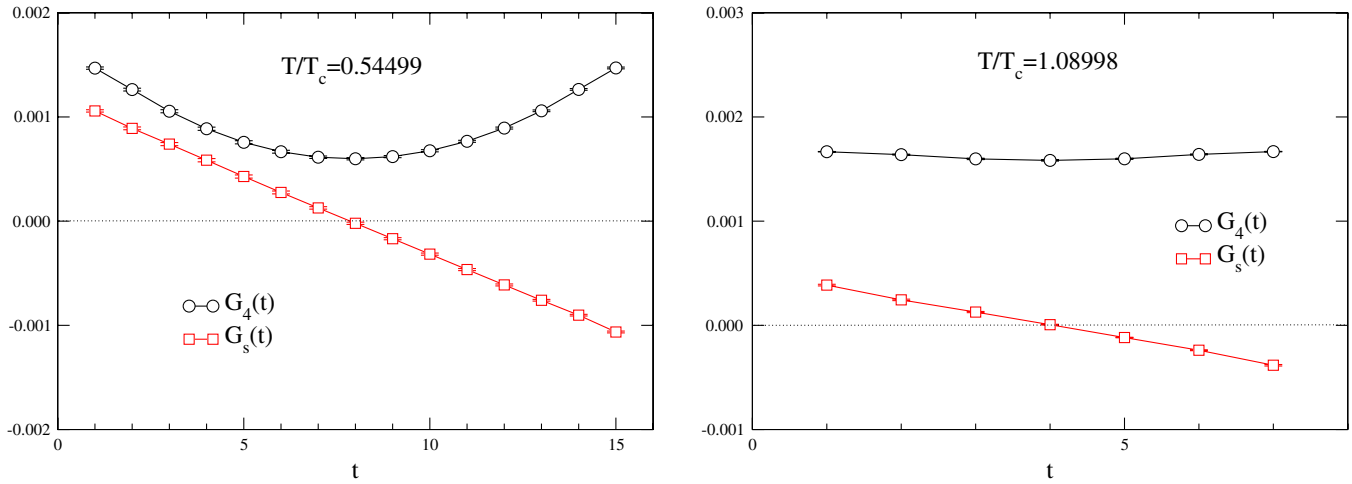

FIG. 1 (color online). The results of quark propagators in the confinement and deconfinement phases. The quark propagator does not produce a significant qualitative change above T_c.

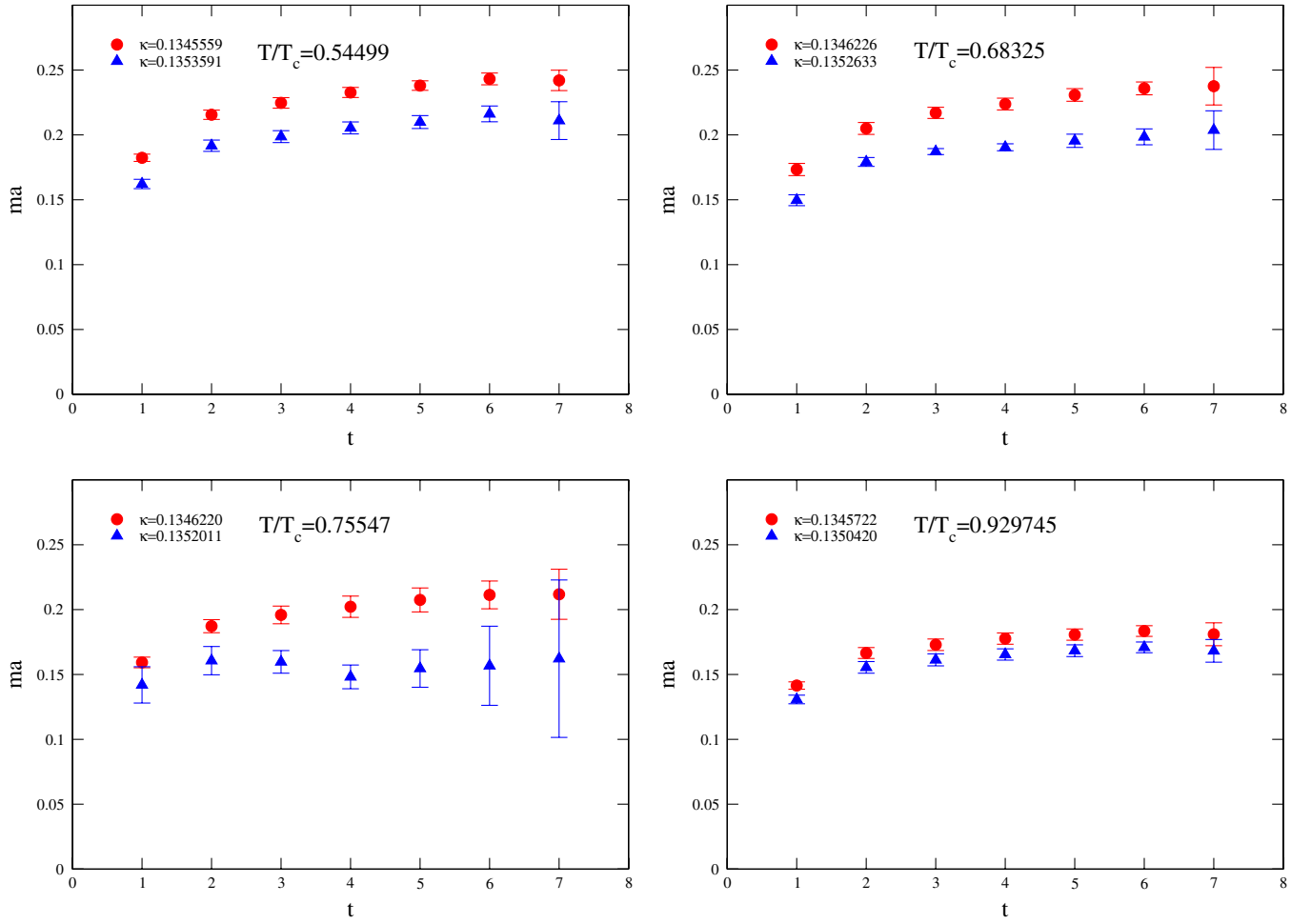

FIG. 2 (color online). Effective masses for the vector part of quark propagators in the confinement phase on the lattice $N_s = 24$ and $N_t = 16$. The upper two figures correspond to the results of $\beta = 6.10$ (left) and $\beta = 6.25$ (right). The lower two figures correspond to the results of $\beta = 6.32$ (left) and $\beta = 6.47$ (right).

B. Volume dependence of effective mass

Figure 4 shows the volume dependence of the effective mass for the vector part. The variation of the spatial-volume size affects the values of the effective masses. In the larger lattice computation ($N_s = 32$), a smaller effective mass than that for the lattice with $N_s = 24$ is obtained. The qualitative feature of the quark propagators does not significantly vary [30].

C. Temperature dependence of the effective mass

Figure 5 shows the temperature dependence of the effective mass in order to look into a qualitative difference near T_c although the effective mass is not well-defined when the spectral function is ill-defined. It is found that m/T_c drops to approximately half value after the QGP phase transition. On the other hand, the values of m/T_c below or above T_c are approximately constant in comparison with the temperature variation. The perturbative formula of the thermal quark mass is given as $m = (1/\sqrt{6})g(T)T$ [31], whose values are plotted also in Fig. 5. Here, the running coupling constant $g(T)$ is defined as

$$g^2(T) = \frac{1}{\beta_0 \ln(\frac{\mu}{\Lambda})^2}\left(1 - \frac{\beta_1}{\beta_0^2}\frac{\ln(\ln(\frac{\mu}{\Lambda})^2)}{\ln(\frac{\mu}{\Lambda})^2}\right), \qquad (12)$$

where the $\beta_0 = 33/48\pi^2$ and $\beta_1 = (34/3)(3/16\pi^2)^2$ [the first two universal coefficients of the renormalization group on $SU(3)$], and the renormalization point μ and the QCD scale Λ are set as $2\pi T$ and $1.03T_c$ [32,33]. The difference between the numerical results and the perturbative value may arise due to $g(T) \sim O(1)$ above T_c. This tendency is also found in the lattice simulation of the gluon screening masses in Ref. [33].

IV. SUMMARY

We studied quark propagators at finite temperature in quenched-lattice simulation in the confinement and decon-

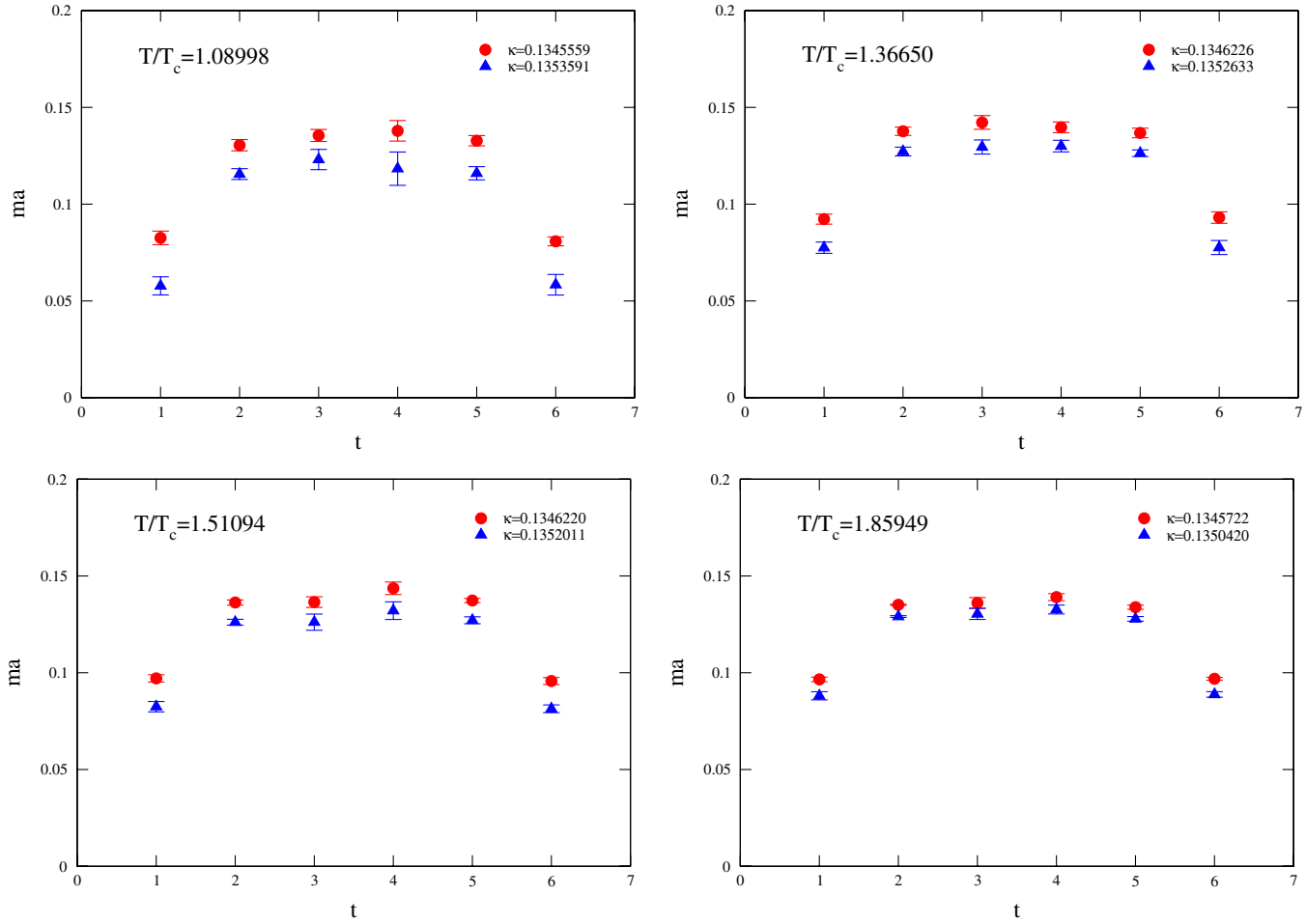

FIG. 3 (color online). Effective masses for the vector part in the deconfinement phase on the lattices of $N_s = 24$ and $N_t = 8$. The upper two figures correspond to the results for $\beta = 6.10$ (left) and $\beta = 6.25$ (right). The lower two figures correspond to the results for $\beta = 6.32$ (left) and $\beta = 6.47$ (right). The effective masses approach a plateau from below with the imaginary time.

finement phases. We employ the plaquette gauge action with $O(a)$ improved clover fermion. The simulations are carried out on several lattice sizes, QCD couplings, quark mass parameters. This enables us to investigate the temperature dependence of the propagators and the effective masses for $T/T_c \sim 0.5$–1.8. In the calculation of the quark propagators the Landau-gauge fixing on the lattice is employed.

Our computations show that there are no significant changes for the quark correlators above and below T_c. Surprisingly, the quarks seem to carry no information about the confinement. However, the effective masses obtained from the vector sector of the quarks changes rapidly only after the phase transition. All the temperature points made here are below $2T_c$ and those thermal masses may not coincide with the perturbative value. Nevertheless, our analyses are not applicable to the scalar sector of the propagators because it may need high temporal resolutions. Since the temporal physical size is limited at finite temperature, i.e., $N_t a = 1/T$, we can not rule out the possibility that the circumstance is not easily improved by brute force.

In this study, we employ rather heavy quark masses, but the behavior of Polyakov lines tells us that the excess free energy diverges in the confinement phase while in the QGP phase it becomes zero, which has been shown by many numerical simulations.

Moreover, in order to understand strongly interacting QGP, we have to do more extensive simulations on larger lattices (for infrared physics) and at higher temperature (for LHC physics). It is also important to search how our conclusion depends on β, N_t and a choice of gauge. Full-QCD simulations are desirable for complete understanding on quark dynamics in both the confinement and deconfinement regions. Besides, computations with other improved actions are complementary to control the discretization effect.

Finally, we point out that the infrared property of the quark propagators has been studied in terms of center vortex mechanism that is responsible for nonperturbative

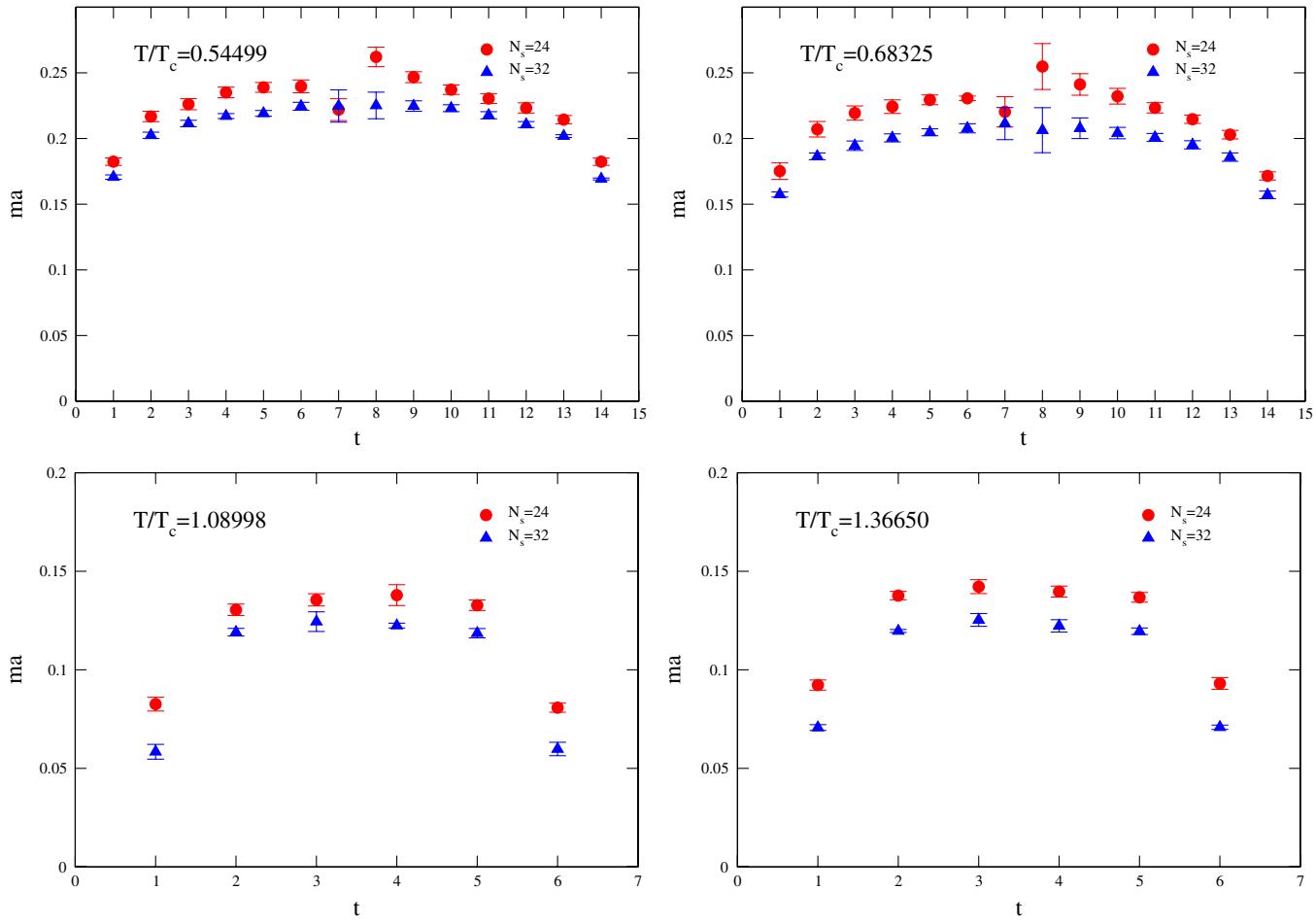

FIG. 4 (color online). Volume dependence of effective masses for the vector part of quark propagators. The upper two figures correspond to the results of the confinement phase with $\beta = 6.10$ (left) and $\beta = 6.25$ (right). The lower two figures correspond to the results of the deconfinement phase with $\beta = 6.10$ (left) and $\beta = 6.25$ (right). All the effective masses decrease as the volume increases, although their dependencies are small.

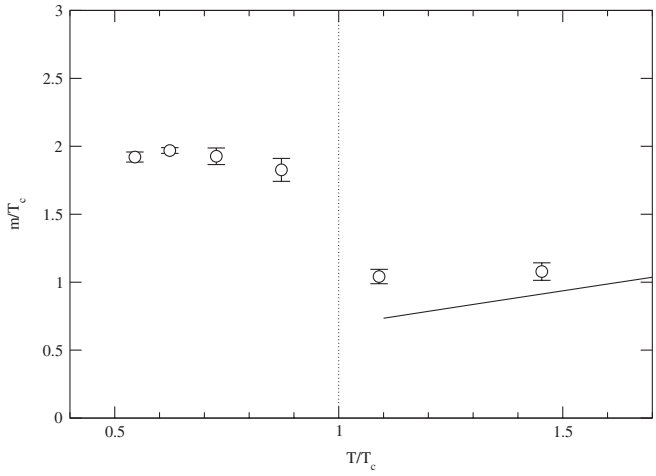

FIG. 5. Dependence of effective masses on the temperature. The solid line stands for the perturbative value. Here, we employ the lattices for $N_s = 32$ and $N_t = 16, 14, 12, 10$ (confinement) and $N_t = 8, 6$ (deconfinement) to vary the temperature. The lattice coupling and the quark mass parameter are taken as $\beta = 6.10$ and $\kappa = 0.1345559$ so as to fix a bare quark mass $m_q/T_c \sim 0.5$ or $m_\pi/m_\rho \sim 0.7$ (~ 0.18 on exp.) which is estimated by the figures in Ref. [38]. The effective masses are determined at intermediate t regions by dropping data on the edges, which results in χ^2/No. of degrees of freedom $\lesssim 1$. m/T_c changes sharply before and after the QGP phase transition.

physics of QCD [34–36]. The gluon dynamics also has been investigated by using center projected lattices in Ref. [37]. These approaches at finite temperature might give a great hint to understand an infrared dynamics of quarks and gluons living in strongly interacting QGP.

ACKNOWLEDGMENTS

We thank Professors M. Kitazawa and F. Karsch for valuable discussions and encouragement. The simulation was carried out on SX-8 at the Research Center for Nuclear Physics, Osaka University, SR11000 at Hiroshima University, RIKEN Super Combined Cluster (RSCC) at Riken, and the kyu-cc at Kyushu University. The work is partially supported by Grants-in-Aid for Scientific Research from Monbu-kagakusyo, Grants No. 17340080 and No. 20340055.

[1] L. D. McLerran and B. Svetitsky, Phys. Lett. **98B**, 195 (1981); Phys. Rev. D **24**, 450 (1981); J. Kuti, J. Polonyi, and K. Szlachanyi, Phys. Lett. **98B**, 199 (1981); J. Engels, F. Karsch, H. Satz, and I. Montvay, Nucl. Phys. **B205**, 545 (1982); For recent progress, see C. DeTar, Proc. Sci. LATTICE2008 (2008) 001.
[2] M. Gyulassy and L. McLerran, Nucl. Phys. **A750**, 30 (2005).
[3] E. Shuryak, Prog. Part. Nucl. Phys. **62**, 48 (2009).
[4] R. Fukuda and T. Kugo, Nucl. Phys. **B117**, 250 (1976).
[5] V. N. Gribov, Eur. Phys. J. C **10**, 91 (1999).
[6] R. Alkofer, W. Detmold, C. S. Fischer, and P. Maris, Phys. Rev. D **70**, 014014 (2004).
[7] A. Krassnigg and C. D. Roberts, Nucl. Phys. **A737**, 7 (2004).
[8] P. O. Bowman, U. M. Heller, D. B. Leinweber, A. G. Williams, and J. B. Zhang, *Lattice Hadron Physics*, Lecture Notes (Springer-Verlag, Berlin, 2005).
[9] P. O. Bowman, U. M. Heller, D. B. Leinweber, M. B. Parappilly, A. G. Williams, and J. Zhang, Phys. Rev. D **71**, 054507 (2005).
[10] M. B. Parappilly, P. O. Bowman, U. M. Heller, D. B. Leinweber, A. G. Williams, and J. B. Zhang, Phys. Rev. D **73**, 054504 (2006).
[11] W. Kamleh, P. O. Bowman, D. B. Leinweber, A. G. Williams, and J. Zhang, Phys. Rev. D **76**, 094501 (2007).
[12] P. O. Bowman, K. Langfeld, D. B. Leinweber, A. Cais, A. Sternbeck, L. Smekal, and A. G. Williams, Phys. Rev. D **78**, 054509 (2008).
[13] H. Nakajima and S. Furui, Proc. Sci., LATTICE2005 (2005) 302.
[14] S. Furui and H. Nakajima, Phys. Rev. D **73**, 074503 (2006).
[15] S. Furui, Few-Body Syst. **45**, 51 (2009); **46**, 73(E) (2009).
[16] G. Boyd, F. Karsch, and S. Gupta, Nucl. Phys. **B385**, 481 (1992).
[17] P. Petreczky, F. Karsch, E. Laermann, S. Stickan, and I. Wetzorke, Nucl. Phys. B, Proc. Suppl. **106**, 513 (2002).
[18] F. Karsch and M. Kitazawa, Phys. Lett. B **658**, 45 (2007); Phys. Rev. D **80**, 056001 (2009).
[19] B. Sheikholeslami and R. Wohlert, Nucl. Phys. **B259**, 572 (1985).
[20] Ph. de Forcrand *et al.* (QCD-TARO Collaboration), Phys. Rev. D **63**, 054501 (2001).
[21] Y. Hidaka and R. D. Pisarski, Phys. Rev. D **78**, 071501(R) (2008); Nucl. Phys. **A820**, 91C (2009).
[22] A. Nakamura and S. Sakai, Phys. Rev. Lett. **94**, 072305 (2005).
[23] J. Liao and E. Shuryak, Phys. Rev. C **75**, 054907 (2007).
[24] M. N. Chernodub and V. I. Zakharov, Phys. Rev. Lett. **98**, 082002 (2007).
[25] M. N. Chernodub, A. Nakamura, and V. I. Zakharov, Phys. Rev. D **78**, 074021 (2008).
[26] R. Alkofer, W. Detmold, C. S. Fischer, and P. Maris, Phys. Rev. D **70**, 014014 (2004).
[27] N. Nakanishi and I. Ojima, *Covariant Operator Formalism of Gauge Theory and Quantum Gravity*, Lecture Notes in Physics (World Scientific, Singapore, 1990), Vol. 27.
[28] M. Luscher, S. Sint, R. Sommer, P. Weisz, and U. Wolff, Nucl. Phys. **B491**, 323 (1997).
[29] K. Akemi *et al.* (QCDTARO Collaboration), Phys. Rev. Lett. **71**, 3063 (1993).
[30] A similar result was obtained in Ref. [18] for the heavy quark, although the volume dependence becomes more significant as approaching the chiral limit.
[31] M. Le Bellac, *Thermal Field Theory*, Cambridge Monographs on Mathematical Physics (Cambridge University Press, Cambridge, United Kingdom, 1996).
[32] J. O. Andersen, E. Bratten, and M. Stickland, Phys. Rev. Lett. **83**, 2139 (1999).
[33] A. Nakamura, T. Saito, and S. Sakai, Phys. Rev. D **69**, 014506 (2004); A. Nakamura, I. Pushkina, T. Saito, and S. Sakai, Phys. Lett. B **549**, 133 (2002).
[34] J. Gattnar, C. Gattringer, K. Langfeld, H. Reinhardt, A. Schafer, S. Solbrig, and T. Tok, Nucl. Phys. **B716**, 105 (2005).
[35] M. Faber, J. Greensite, U. M. Heller, R. Hoellwieser, and S. Olejnik, Phys. Rev. D **78**, 054508 (2008).
[36] P. O. Bowman, K. Langfeld, D. B. Leinweber, Al. O'Cais, A. Sternbeck, L. von Smekal, and A. G. Williams, Phys. Rev. D **78**, 054509 (2008).
[37] T. Saito, M. N. Chernodub, Atsushi Nakamura, and V. I. Zakharov, Proc. Sci., LATTICE2009 (2009) 179.
[38] M. Göckeler, R. Horsley, H. Perlt, P. Rakow, G. Schierholz, A. Schiller, and P. Stephenson, Phys. Lett. B **391**, 388 (1997).